Applied Catalysis A: General 482 (2014) 31–37

Contents lists available at ScienceDirect

Applied Catalysis A: General

journal homepage: www.elsevier.com/locate/apcata

Sulfonic acid functionalized deoxycellulose catalysts for glycerol acetylation to fuel additives

Inbae Kim[1], Jaesung Kim[1], Doohwan Lee*

Catalysis and Nanomaterials Laboratory, Department of Chemical Engineering, University of Seoul, Siripdae-gil 13, Jeonnong-dong, Dongdaemun-gu, Seoul 130-743 Republic of Korea

ARTICLE INFO

Article history:
Received 22 January 2014
Received in revised form 12 May 2014
Accepted 16 May 2014
Available online 27 May 2014

Keywords:
Cellulose
Glycerol acetylation
Heterogeneous catalyst
Sulfonic acid functionalization
Renewable energy

ABSTRACT

Various forms of sulfonic acid (—SO_3H) functionalized cellulose-based heterogeneous catalysts were prepared, and their properties on glycerol acetylation reactions to mono-, di-, and triacetin products were investigated. Superior catalytic activity and stability for the reactions was observed on SO_3H-NDOC catalyst that is obtained by (i) crosslinking of the cellulose units with epichlorohydrin into a three-dimensionally-networked deoxycellulose-matrix and (ii) sulfonic acid functionalization on the crosslinked deoxycellulose support via C—S atomic linkages (—C—SO_3H). It was found that sulfonic acid functionalization via an ether type O—S atomic linkage (—C—O—SO_3H) or the direct utilization of the pristine cellulose support without a fortification by crosslinking led to significant deactivation of the catalysts by substantial acidity loss. The intrinsic glycerol conversion turnover rate on SO_3H-NDOC was comparable to that of commercial Amberlyst-15 solid resin, demonstrating the effectiveness of this renewable cellulose-derived heterogeneous catalyst for glycerol acetylation to fuel additives.

1. Introduction

Cellulose is abundant natural resource that is being utilized as a raw material for various value-added products. In recent years, its non-conventional utilization as a feedstock for liquid biofuel and bio-derived chemicals is being extensively explored due to growing concern related to sustainability of the current petroleum-based energy and materials infrastructure [1,2]. In another respect, cellulose is of particular interest as a bio- or eco-friendly alternative for versatile applications in the fields of medical, pharmaceutical, and specialty materials [3]. Cellulose is a natural polymer consisting of three hydroxyl groups per anhydroglucose unit (AGU) that enable functionalization of the structure for use in heterogeneous catalysts. Choplin et al. immobilized a $Pd(OAc)_2$/5-TPPTS [TPPTS = $P(m\text{-}C_6H_4SO_3Na)_3$] catalytic precursor onto cellulose and reported that the resulting material effectively catalyzed an allylic alkylation reaction of (*E*)-cinnamyl ethyl carbonate with morpholine without sizeable leaching of Pd from the catalyst [4]. Shaabani et al. reported a sulfonic acid functionalized cellulose catalyst (SO_3H-Cell) and its effective catalytic properties for the synthesis of α-amino nitriles [5], quinolines [6], and amide and amine derivatives [7]. The SO_3H-Cell catalyst was also effectively applied for the synthesis of 1,4-dihydropyridine by Safari et al. [8] and of 2,4,5-triarylimidazoles by Shingare et al. [9]. These previous studies on the SO_3H-Cell catalyst are attractive considering its reasonable stability under reaction conditions that appear to be hostile to the integrity of the catalysts. Specifically, the presence of acids, water, and alcohols in reactants/products, or elevated reaction temperatures reported therein may facilitate hydrolysis of the cellulose and the immobilized sulfonic acid group.

Here we report the first synthesis and properties of a structurally-fortified sulfonic acid functionalized deoxycellulose-based catalyst that is constructed by immobilization of —SO_3H groups onto a three-dimensionally networked deoxycellulose matrix via C—S atomic linkages (referred to here as SO_3H-NDOC). The catalyst was applied for glycerol acetylation with acetic acid for the production of mono-, di-, and triacetin (Scheme 1). This catalytic transformation is considered to be an effective route for utilization of the excessive glycerol byproduct obtained from biodiesel synthesis [10,11]. The reaction can be conducted in the liquid phase at moderate temperatures below 373 K, and the acetylated-glycerol products can be used as value-added fuel additives [12]. Properties of SO_3H-NDOC for the reaction are also compared with sulfonic acid functionalized deoxycellulose (SO_3H-DOC) and cellulose (SO_3H-Cell) catalysts as well as commercial Amberlyst-15 acid resin.

---

* Corresponding author. Tel.: +82 2 6490 2371; fax: +82 2 6490 2364.
E-mail address: dolee@uos.ac.kr (D. Lee).

[1] I. Kim and J. Kim equally contributed to this work.

http://dx.doi.org/10.1016/j.apcata.2014.05.018
0926-860X/

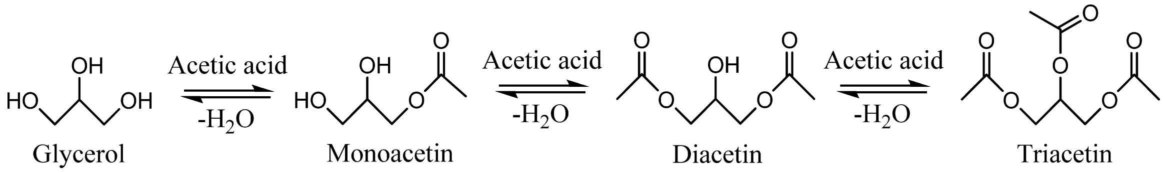

Scheme 1. Glycerol acetylation with acetic acid to mono-, di-, and triacetin products.

2. Experimental

2.1. Catalysts preparation

2.1.1. Preparation of SO_3H-Cell catalyst

The SO_3H-Cell catalyst was prepared according to the procedure reported by Safari et al. [8]. Briefly, 5 g of microcrystalline cellulose powder (Alfa, particle size <220 μm) was dispersed in 20 ml of *n*-hexane (Aldrich, HPLC grade) with vigorous stirring in an ice bath, and then 9 mmol of chlorosulfonic acid (Aldrich, 99%) was added slowly in a drop-wise manner for 2 h. The resulting mixture was stirred for an additional 2 h, filtered, and washed with acetonitrile (Aldrich, 99.9%). The SO_3H-Cell sample was dried at 313 K in a convection oven for 12 h.

2.1.2. Preparation of SO_3H-DOC catalyst

The sulfonic acid functionalized deoxycellulose catalyst (SO_3H-DOC) was prepared as shown in Scheme 2(a). In the first step, chlorodeoxycellulose (Cl–DOC) was prepared according to the procedure reported by Takagai et al. [13]. Briefly, 2 g of the cellulose powder was dispersed in 50 ml of DMF (Junsei, 99.5%) in a reflux condenser equipped flask at 353 K for 2 h with vigorous stirring. Then, 1.8 ml of $SOCl_2$ (Aldrich, 99%) was added and the mixture was stirred for an additional 2 h. The resulting mixture was centrifuged and washed with acetone and deionized water. In the second step, the collected sample was dispersed in 180 ml of NMP (Junsei, 99%) at 343 K for 30 min. The mercaptodeoxycellulose (SH–DOC) was obtained by adding 4 g of NaHS (Aldrich) with stirring for 3 h. Then, the mixture was centrifuged and washed with copious amounts of H_2O. In the final step, the SO_3H-DOC was obtained after treating the collected SH–DOC in 100 ml of H_2O_2 (Junsei, 30%) at room temperature for 5 h with stirring. The resulting catalyst powder was centrifuged, washed with H_2O, and dried in a vacuum oven at 313 K. The acidity on the samples did not increase by an additional acidification treatment with 0.1 M HNO_3 solution for 12 h indicating that the resulting sulfonic acid groups were completely protonated.

2.1.3. Preparation of SO_3H-NDOC catalyst

The sulfonic acid functionalized three-dimensionally-networked deoxycellulose catalyst (SO_3H-NDOC) was synthesized as displayed in Scheme 2(b). The synthesis procedure and method including the —Cl [13], —SH, and —SO_3H functionalization were the same to those applied for SO_3H-DOC, except that the functionalization was conducted on the networked cellulose matrix (NDOC) which was prepared by crosslinking of cellulose units with epichlorohydrin (EP) as a linking agent. Briefly, 4 g of microcrystalline cellulose particles was dispersed in 160 ml of 2.4 M NaOH aqueous solution for 10 min. The dispersed cellulose particles were completely dissolved into a homogeneous solution after a low temperature treatment in a liquid N_2 bath for 15 min. The resulting cellulose solution was heated to 313 K, and various amounts of EP (Alfa, 99%) were added with vigorously stirring for 2 or 12 h. The product was centrifuged, washed with copious amounts of water, and dried in a vacuum oven at 323 K.

2.2. Characterization of the catalysts

Brönsted acidity of the samples was characterized by the neutralization titration method [14]. In the typical procedure, 0.05 g of catalyst powder was treated with 20 ml of 1.0 M aqueous NaCl solution for 1 h at room temperature with sonication. A longer treatment had no effect on acidity of the samples. After centrifugal separation, the supernatant solution was treated with a 0.01 M aqueous NaOH solution using phenolphthalein as the neutralization indicator. The method does not titrate the hydroxyl or thiol groups as was confirmed from the measurements conducted on the pristine cellulose and SH–DOC samples. Carbon and sulfur contents in the dried catalyst samples were obtained by elemental analysis (Flash 2000 CHNS analyzer, Thermo Scientific). The structures of pristine cellulose, crosslinked deoxycellulose (NDOC), and SO_3H-NDOC samples were analyzed by Fourier-transform infrared spectroscopy (Nicolet 6700, Thermo Scientific). The IR spectra were obtained from thin wafers that were prepared by pelletizing mixture powders of the dried sample and KBr. The porosity of the samples was indirectly characterized by measuring the swelling of the samples in the presence of water [15]. For the measurement, 0.15 g of dried catalyst was soaked into 20 ml of deionized water for 48 h at room temperature and separated by centrifugation. The degree of swelling was defined as a weight ratio of water absorbed into the sample to the initial weight of dried catalyst, described as

$$S_w = \frac{W - W_0}{W_0} \tag{1}$$

where S_w is the degree of swelling, W is the weight of cellulose catalyst after water absorption, and W_0 is the initial weight of dried catalyst.

2.3. Glycerol acetylation reaction

Glycerol acetylation with acetic acid was conducted in a 500 ml three-neck round-bottom flask equipped with a reflux condenser at atmospheric pressure. All the catalysts were utilized as powders. Amberlyst-15 (Rohm & Hass) beads were crushed into powders with sizes between 125 and 180 μm. The reactor was placed in a heating mantle, and the inner temperature of the reactor was isothermally maintained by PID control. In the typical procedure, 78.2 g of acetic acid (Alfa, 99.7%) and 1.0 g of the catalyst powder were placed into the reactor at a constant temperature of 353 K, and then 20.0 g of glycerol (Alfa, HPLC grade) at the same temperature was added with stirring. The products were sampled periodically during the reaction using a micro-syringe and were analyzed with a flame ionization detector (FID) equipped gas chromatograph (Agilent 7890A). After each reaction batch, the catalyst was collected by centrifugation, washed with methanol (Amberlyst-15) or deionized water (SO_3H-Cell, SO_3H-DOC, SO_3H-NDOC) several times, and dried in a vacuum oven at 323 K for 20 h for utilization in the subsequent reaction batch. Glycerol conversion turnover rate (TOR) to combined di- and triacetin products on SO_3H-NDOC and Amberlyst-15 was obtained according to the following equation:

$$\text{Glycerol TOR} = \frac{\text{Production rate for di- and triacetin (mmol g}^{-1}\,\text{h}^{-1})}{\text{Acidity on the catalyst (mmol g}^{-1})} \tag{2}$$

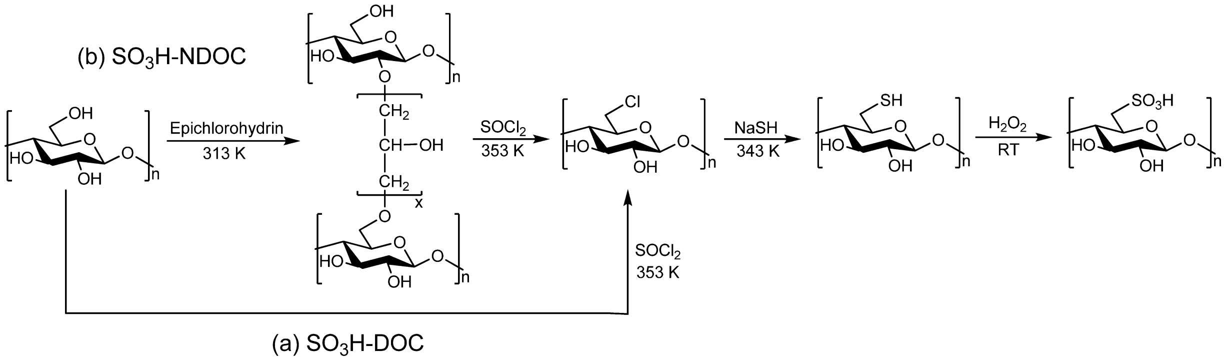

Scheme 2. Synthesis procedure of (a) sulfonic acid functionalized deoxycellulose (SO_3H-DOC) and (b) sulfonic acid functionalized three-dimensionally networked deoxycellulose (SO_3H-NDOC) catalyst.

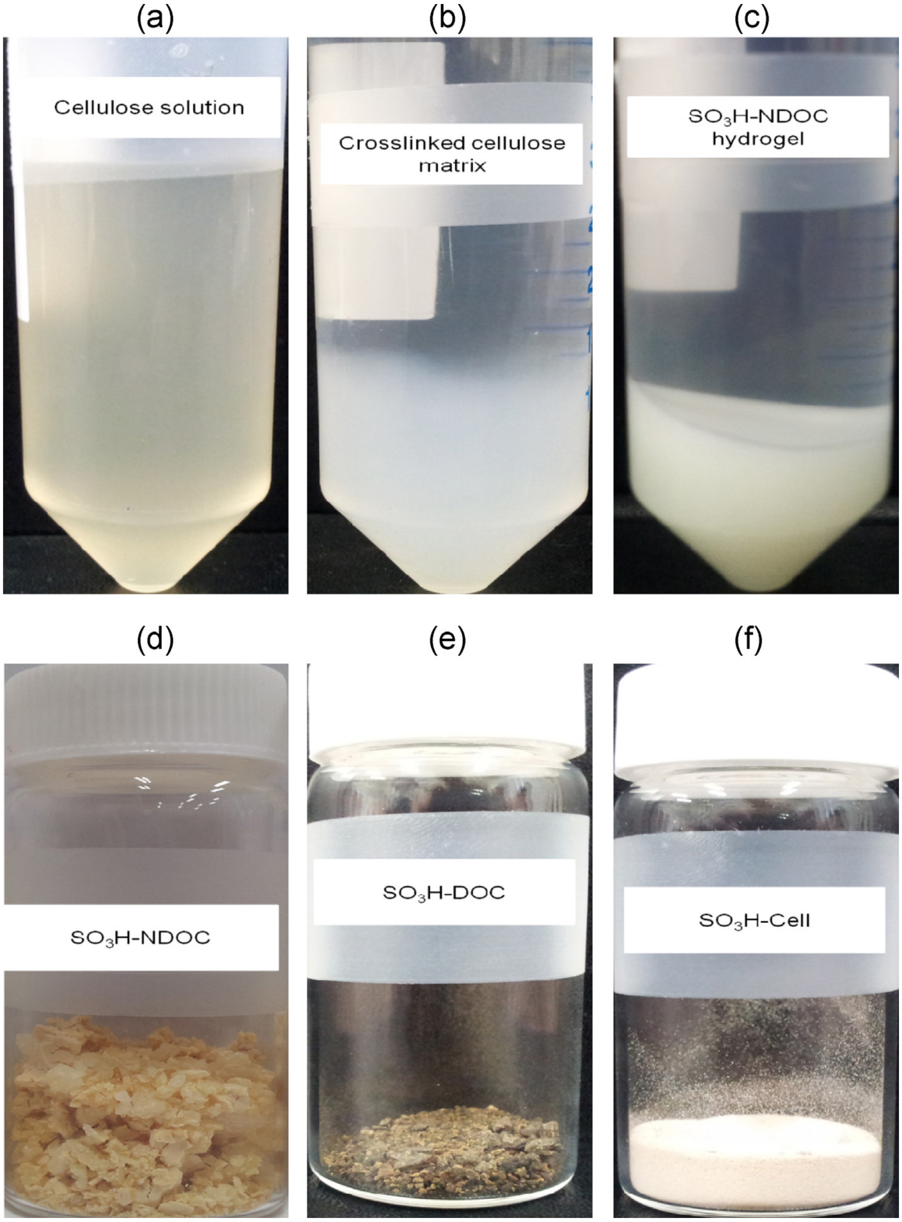

Fig. 1. Photographs of the synthesis intermediates for SO_3H-NDOC and the final forms of cellulose-based catalysts; (a) cellulose solution, (b) crosslinked cellulose matrix, (c) SO_3H-NDOC hydrogel, (d) SO_3H-NDOC after drying, (e) SO_3H-DOC after drying, (f) SO_3H-Cell after drying.

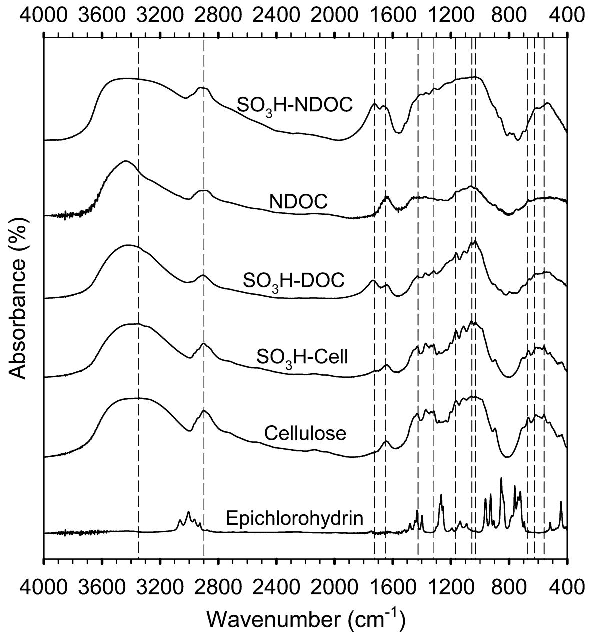

Fig. 2. FT-IR spectra of SO_3H-NDOC, NDOC, SO_3H-DOC, SO_3H-Cell, pristine cellulose, and epichlorohydrin (EP).

3. Results and discussion

3.1. Characteristics of the catalysts

Photographs of homogenous cellulose solution, crosslinked cellulose matrix, and the final forms of SO_3H-NDOC catalyst (before and after drying) described in Scheme 2 are presented in Fig. 1 (photographs of the Cl-NDOC and SH-NDOC can be found in Supplementary information, Fig. S1). The final dried form of SO_3H-DOC and SO_3H-Cell catalysts are also displayed for comparison. The results clearly demonstrate the formation of a cellulose hydrogel by networking of the dispersed cellulose units, where the resulting matrix was stable under the subsequent deoxy-chlorination, thiolation, and oxidation steps for the preparation of SO_3H-NDOC catalyst. In contrast, the deoxychlorination of homogenously dispersed cellulose for SO_3H-DOC that was conducted without prior crosslinking of the cellulose chains resulted in precipitation of the chlorinated deoxycellulose powders with completely different morphological features. The FT-IR absorption spectra of SO_3H-NDOC, NDOC, SO_3H-DOC, SO_3H-Cell, pristine cellulose, and EP shown in Fig. 2 evidently indicate the crosslinking of cellulose units (NDOC) and the formation of sulfonic acid functional group on NDOC support via C—S atomic linkages (—C—SO_3H). On pristine cellulose, the characteristic IR absorption bands of cellulose including —OH (3346 cm^{-1}) and C—H (2899) stretching, absorbed water in cellulose (1644), —OH inplane deformation (1431–1319), C—O antisymmetric bridge stretching (1164), and anhydroglucose ring stretching (1059, 667, 559) vibration were identified [16–18]. The overall spectral features of NDOC, and SO_3H-NDOC samples were similar to that of pristine cellulose, but the absorption bands of —OH inplane deformation, C—O antisymmetric bridge stretching, and anhydroglucose ring stretching vibrations were not observed. Differently, these IR bands were clearly observed on SO_3H-Cell and SO_3H-DOC samples. The results were reasonable and support the formation of three dimensionally networked cellulose chains in NDOC and SO_3H-NDOC, because the crosslinking of cellulose units would substantially hinder the vibration of anhydroglucose ring structures. Notice that the characteristic absorption bands of epoxy ring (1267, 854) and C—Cl (761) stretching vibration presented in EP were not observed in NDOC [19]. The substitution of —Cl functional groups on Cl-NDOC was confirmed with the characteristic C—Cl stretching vibration (749, 719 cm^{-1}) [20], and this did not appear on SH-NDOC and SO_3H-NDOC samples (the IR spectra of Cl-NDOC and SH-NDOC are shown in Fig. S2). The formation of sulfonic acid functional group on DOC and NDOC via C—S atomic linkage (—C—SO_3H) was confirmed in SO_3H-DOC and SO_3H-NDOC catalyst, on which C—SO_3H (620 cm^{-1}) and S=O (1035) stretching vibrations were observed [14,21]. In addition, the C=O stretching vibration (1724 cm^{-1}) band appeared on the sample indicated that some parts of unsubstituted hydroxyl groups on SO_3H-DOC and SO_3H-NDOC samples oxidized further into ketone groups [22].

Properties of the resulting SO_3H-NDOC are different from those of SO_3H-DOC and SO_3H-Cell, as compared in Table 1, in which three SO_3H-NDOC samples prepared at varied EP/AGU mole ratios and crosslinking reaction time are displayed. The degree of swelling, which is indicative of the porosity of the sample, increased by approximately 140% with an increase in crosslinking time from 2 h to 12 h at a EP/AGU ratio of 10. Noticed that EP does not homogeneously crosslink and was used in excess amounts in the preparation. An increase in the EP/AGU ratio from 10 to 15 did not affect the degree of swelling. The acidities of SO_3H-NDOC samples were lower than that of SO_3H-DOC, which was reasonable considering that some parts of the hydroxyl groups presented in the pristine cellulose units were consumed by crosslinking with EP, resulting in a decrease in the number of sites available for sulfonic acid functionalization. The acidity of the SO_3H-Cell was low because the–SO_3H substitution on this catalyst could occur only on the near surface of the microcrystalline cellulose support. It also should be noted that the sulfonic acid functional groups on SO_3H-NDOC and SO_3H-DOC were linked to the cellulose matrix via C—S atomic bonding, whereas those on the SO_3H-Cell were linked to the matrix via C—O—S atomic bonding. As a consequence, their stability against hydrolysis is significantly different, as will be discussed. Sulfur contents on the —SO_3H functionalized deoxycellulose-based catalysts were higher than the acidity on the samples, indicating that a sizable portion of the substituted —SH species remained in the matrix without conversion to the final —SO_3H group.

Table 1
Properties and synthesis conditions of the sulfonic acid functionalized cellulose-based catalysts.

Catalyst	Acidity[a] (mmol g_{cat}^{-1})	Sulfur content[b] (mmol-S g_{cat}^{-1})	Sulfur/carbon atomic ratio[b] (%)	Degree of swelling	EP/AGU molar ratio	Crosslinking reaction time (h)
SO_3H-NDOC-1	0.37	1.8	5.3	2.4	10	2
SO_3H-NDOC-2	0.97	2.4	7.6	4.4	10	12
SO_3H-NDOC-3	0.84	3.0	9.7	3.4	15	12
SO_3H-DOC	1.84	2.9	9.9	3.3	–	–
SO_3H-Cell	0.62	0.6	1.1	2.1	–	–
Amberlyst-15	4.77	–	–	–	–	–

EP: epicholorohydrin, AGU: anhydroglucose unit in cellulose.

[a] Estimated by neutralization titration method.

[b] Estimated by elemental analysis.

Table 2
Glycerol conversion and product selectivity on the catalysts at 353 K for 3 h of batch reaction.

Catalyst	Glycerol conversion (%)	Glycerol conversion to DA and TA (%)	Product selectivity (%)		
			MA	DA	TA
SO_3H-NDOC	98	51	48	45	7
SO_3H-DOC	99	56	44	48	8
SO_3H-Cell	93	26	72	26	2
Amberlyst-15	100	60	40	54	6
Blank	49	3	94	6	0

Reactant feed condition: $C_2H_4O_2/C_3H_8O_3 = 6$, catalyst loading amount = 5 wt% based on the glycerol feed, MA = monoacetin, DA = diacetin, TA = triacetin.

3.2. Catalytic properties for glycerol acetylation reaction

Glycerol conversion and product selectivity on the sulfonic acid functionalized cellulose based catalysts obtained at 353 K for 3 h in batch reactions are displayed in Table 2. The SO_3H-NDOC catalyst that was utilized for the reaction was the SO_3H-NDOC-2 sample shown in Table 1, and it will be used and discussed hereafter. The results on the commercial Amberlyst-15 acid resin catalyst are also shown for comparison. A blank batch reaction conducted without catalyst exhibited a considerable glycerol conversion with exclusive product selectivity toward monoacetin, reflecting the facile reaction kinetics toward monoacetin and the thermodynamic characteristic that the Gibbs free energy for formation of 1-monoacetin is substantially lower than those of 1,3-diacetin and triacetin [23]. Therefore, assessment of catalytic activity of the samples was conducted based on the level of glycerol conversion toward combined di- and triacetin products. The results indicated that SO_3H-NDOC and SO_3H-DOC catalysts demonstrated nearly equivalent catalytic activity and product selectivity to the commercial Amberlyst-15 benchmarking catalyst. The comparatively low glycerol conversion toward di- and triacetin products on SO_3H-Cell reflected its low catalytic activity, mainly due to the relatively low acidity on the sample. The high glycerol conversion observed on SO_3H-DOC was due to its high acidity and occurrence of homogenous reaction as will be discussed with the structure stability of these catalysts.

3.3. Stability of the catalysts

Stability of the catalysts was investigated by conducting consecutive batch reactions utilizing the spent catalysts. Fig. 3 displays glycerol conversion and product selectivity on SO_3H-DOC, SO_3H-NDOC, SO_3H-Cell, and Amberlyst-15 catalysts as a function of time for the consecutive reaction batches at 353 K (catalyst loading = 5 wt% based on the glycerol feed amount, $C_2H_4O_2/C_3H_8O_3$ molar ratio = 6). Fig. 4 shows the results in which glycerol conversion to di- and triacetin products on the catalysts are displayed for each consecutive batch run. These results collectively indicate the superior stability of SO_3H-NDOC catalyst for the reaction to SO_3H-DOC and SO_3H-Cell counterparts, wherein limited deactivation occurred only in the first reaction batch. Conversely, continuous and substantial deactivation occurred on SO_3H-DOC and SO_3H-Cell catalysts throughout the consecutive batch runs. The main reasons for deactivation of these catalysts are different, as evidenced by the evolution of catalyst acidity. Table 3 shows the acidity and sulfur contents on the samples that were measured prior to each consecutive batch reaction. The results clearly suggest that the deactivation on SO_3H-Cell occurred due to significant acidity loss throughout the consecutive batch runs. This is reasonable considering that the ether type atomic bonding ($-C-O-SO_3H$) between the SO_3H group and the cellulose matrix is prone to be weak under hydrolysis conditions in the presence of acid, which led to the removal of the acid groups from the cellulose matrix into molecular sulfuric acid species [24,25]. In contrast, limited loss of acidity and sulfur content occurred on SO_3H-NDOC only through the first reaction batch, demonstrating that the–SO_3H group immobilized on the NDOC matrix via a C—S atomic linkage ($-C-SO_3H$) was stable against the hydrolysis reaction environment. The slight acidity loss at the first reaction batch appears to be due to the removal of some sulfonic acid species that were unstably anchored on the deoxycellulose matrix. It was also confirmed by the occurrence of homogeneous reactions (353 K) in the recovered reactants by filtration of the solid catalysts (after 1 h of the 1st reaction batch) as shown in Fig. 5. The results indicated that glycerol conversion to di- and triacetin on SO_3H-NDOC, SO_3H-DOC, and SO_3H-Cell catalysts increased without these solid acids due to the presence of the acid species hydrolyzed or defragmented from the catalysts during the first reaction batch. The constructive effects of the deoxycellulose crosslinking on SO_3H-NDOC were clear when the evolution of glycerol conversion through the consecutive batch runs on this catalyst was compared to that on SO_3H-DOC, as shown in Fig. 4. Although the stable C—S atomic linkage between the deoxycellulose support and $-SO_3H$ functional group also formed on SO_3H-DOC, substantial deactivation of the catalyst occurred as evidenced by the decrease in glycerol conversion throughout consecutive reaction batches. Concomitantly, it was found that acidity on SO_3H-DOC declined sharply after the first reaction batch by approximately 67% and showed only a slight decrease with the subsequent batch runs. The results suggest that, when the structure was not fortified by an extensive crosslinking of the deoxycellulose matrix, a substantial loss of the $-SO_3H$ immobilized deoxycellulose occurs as fragments from the catalyst surface resulting in catalyst deactivation. The sharp decline in acidity during the first reaction batch was reasonable considering that the concentration of sulfonic acid functional groups was expected to be higher on the near surface of SO_3H-DOC. The continuous decrease in glycerol conversion after the second reaction batches without a sizeable acidity loss on SO_3H-DOC suggested that the structure densification affected the reaction kinetics by limiting the mass transfer. We observed that a significant densification and solidification of SO_3H-DOC occurred after washing and drying of the spent catalyst throughout the consecutive reaction batches (SEM micrographs are shown in Supplementary information, Fig. S3). Agglomeration and structure densification of crystalline celluloses by drying due to enhanced molecular contacts of cellulose chains has been reported [26], which agree well with the results obtained in this work.

Table 3
Acidity (mmol-H^+ g_{cat}^{-1}) and sulfur contents[a] (mmol-S g_{cat}^{-1}) on the catalysts measured prior to each reaction batch.

Catalyst	Reaction batch			
	1st	2nd	3rd	4th
SO_3H-NDOC	0.97 (2.4)	0.71	0.74 (1.8)	0.70 (1.6)
SO_3H-DOC	1.84 (2.9)	0.63 (1.1)	0.63 (1.3)	0.56 (1.1)
SO_3H-Cell	0.62 (0.6)	0.11	0.04	0.02
Amberlyst-15	4.77	4.65	4.46	4.50

[a] Sulfur contents are shown in parenthesis.

The extensive study on sulfonic acid functionalized cellulose-based catalysts in this work collectively suggests that (i) the

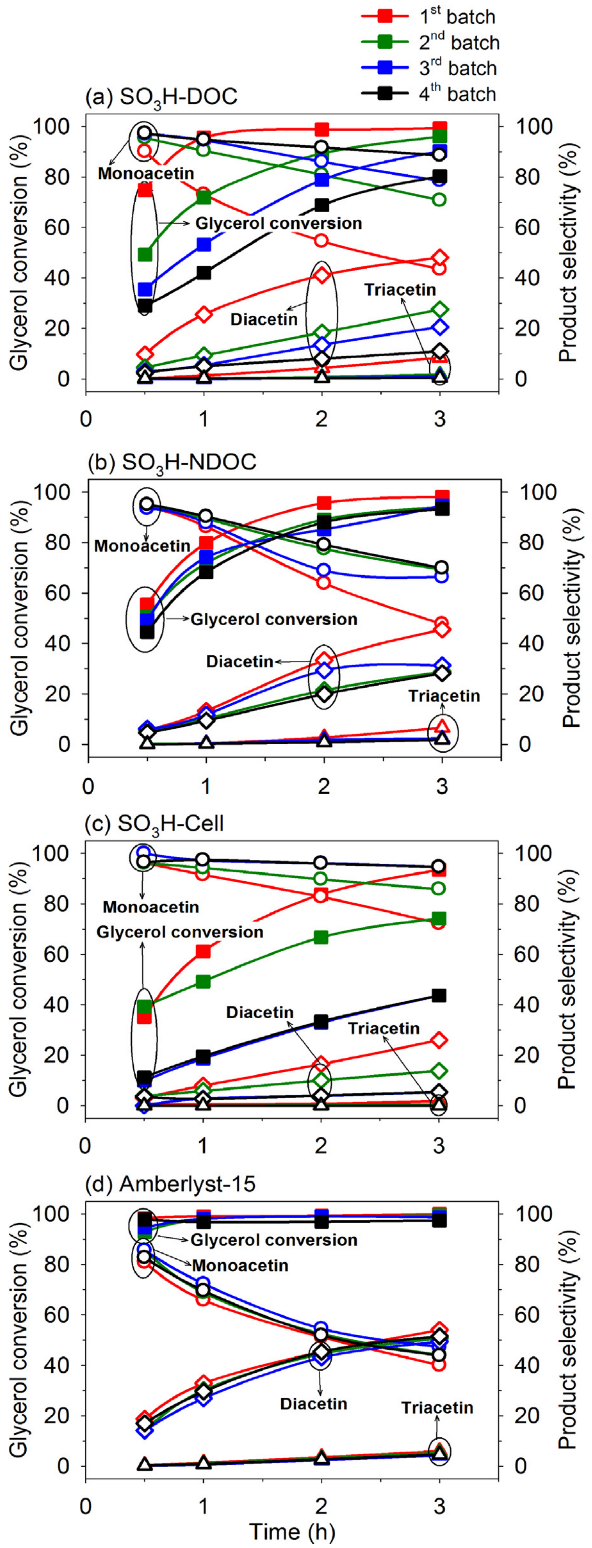

Fig. 3. Glycerol conversion and product selectivity on SO_3H-DOC, SO_3H-NDOC, SO_3H-Cell, and Amberlyst-15 catalysts as a function of time for the consecutive reaction batches at 353 K (red: 1st, green: 2nd, blue: 3rd, black: 4th batch, catalyst loading = 5 wt% based on the glycerol feed, $C_2H_4O_2/C_3H_8O_3$ molar ratio = 6). (For interpretation of the references to color in this figure legend, the reader is referred to the web version of this article.)

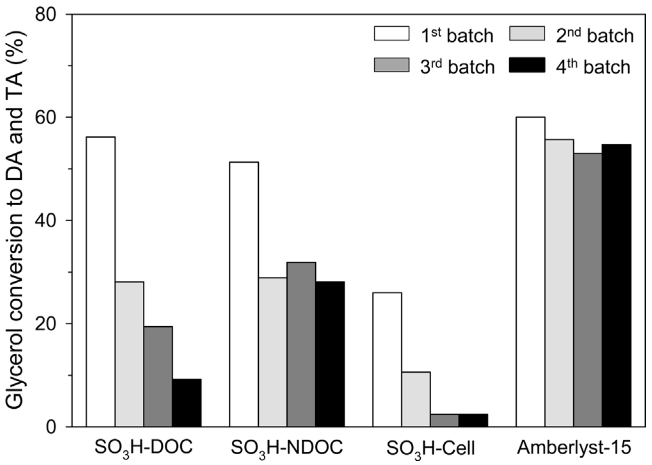

Fig. 4. Glycerol conversion to diacetin (DA) and triacetin (TA) products on the catalyst at 353 K for 3 h of each consecutive batch run (catalyst loading = 5 wt% based on the glycerol feed, $C_2H_4O_2/C_3H_8O_3$ molar ratio = 6).

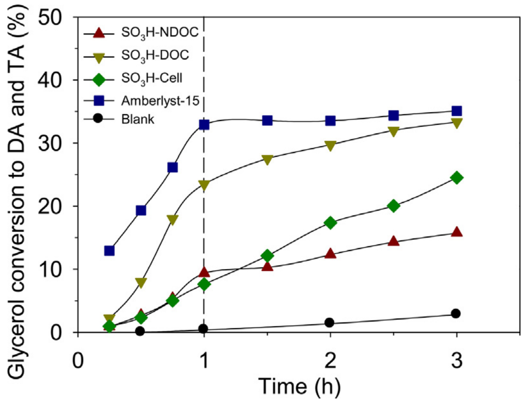

Fig. 5. Glycerol conversion to di- (DA) and triacetin (TA) at 353 K as a function of time. The reactions were initially conducted with the catalysts (5 wt%, $C_2H_4O_2/C_3H_8O_3$ molar ratio = 6) for 1 h, and then the solid catalysts was removed from the reactants by filtration).

C—S atomic linkage between the deoxycellulose matrix and —SO_3H functional group and (ii) the extensive crosslinking among the deoxycellulose units on SO_3H-NDOC catalyst effectively delivered superior catalytic activity and stability for glycerol acetylation reactions. The intrinsic glycerol conversion turnover rates (TOR) to combined di- and triacetin products on SO_3H-NDOC and Amberlyst-15, obtained for the results on the 4th batch shown in Fig. 4, were similar with values of 29.5 and 14.5 h^{-1}, respectively. These results demonstrated that the sulfonic acid functionalized three-dimensionally-networked deoxycellulose (SO_3H-NDOC) effectively catalyzed glycerol acetylation reactions with high stability and can be applied to similar acid catalyzed reactions. The effects of structure and physicochemical property of crosslinking molecules, degree of crosslinking, and density of the acid sites in SO_3H-NDOC catalyst have not investigated in detail in this work, although they can have substantial effects on the reaction rates and internal mass transport through the catalysts. On acid resin catalysts, it was reported that extensive crosslinking negatively affected to the glycerol acetylation reaction due to the mass transfer limitation [27]. However, some extents of cross-linkages between the cellulose chains appear to be necessary for the cellulose-based catalysts that can provide free spaces accessible for the reactant species and also effectively prevent agglomeration and densification of the overall structure.

4. Conclusions

The sulfonic acid (—SO_3H) functionalized three-dimensionally-networked deoxycellulose catalyst (SO_3H-NDOC) prepared in this work demonstrated that (i) the reinforcement of deoxycellulose chains by crosslinking into a networked structure inhibited dissolution and densification of the cellulose matrix, and (ii) the immobilization of —SO_3H functional groups on the support via C—S atomic linkages stabilized the functional groups preventing acidity loss on the catalyst. SO_3H-NDOC effectively catalyzed the glycerol acetylation reactions with an intrinsic conversion rate toward di- and triacetin products comparable to that on commercial Amberlyst-15 solid acid resin. Stability of SO_3H-NDOC catalyst was excellent, exhibiting no sizable deactivation after the first reaction batch. In this work, we mainly investigated the structure to property relations of cellulose-based sulfonic acid catalysts for glycerol acetylation reactions. Although SO_3H-NDOC demonstrated high catalytic property and stability for the reactions, the preparation of the materials may require environmentally benign alternative approaches because the method applied in this work utilized various reagents in the multistep synthesis procedure.

Acknowledgments

The authors acknowledge support from the Korea Research Foundation (KRF 2011-0010095) and the human resources development program of the Korea Institute of Energy Technology Evaluation and Planning (KETEP) under a grant funded by the Korea Government Ministry of Trade, Industry, and Energy (2012-4010203260).

Appendix A. Supplementary data

Supplementary data associated with this article can be found, in the online version, at http://dx.doi.org/10.1016/j.apcata.2014.05.018.

References

[1] J.N. Chheda, G.W. Huber, J.A. Dumesic, Angew. Chem. Int. Ed. Engl. 46 (2007) 7164–7183.
[2] A. Corma Canos, S. Iborra, A. Velty, Chem. Rev. 107 (2007) 2411–2502.
[3] R.J. Moon, A. Martini, J. Nairn, J. Simonsen, J. Youngblood, Chem. Soc. Rev. 40 (2011) 3941–3994.
[4] F. Quignard, A. Choplin, Chem. Commun. (2001) 21–22.
[5] A. Shaabani, A. Maleki, Appl. Catal., A: Gen. 331 (2007) 149–151.
[6] A. Shaabani, A. Rahmati, Z. Badri, Catal. Commun. 9 (2008) 13–16.
[7] H. Mofakham, Z. Hezarkhani, A. Shaabani, J. Mol. Catal. A: Chem. 360 (2012) 26–34.
[8] J. Safari, S.H. Banitaba, S.D. Khalili, J. Mol. Catal. A: Chem. 335 (2011) 46–50.
[9] K.F. Shelke, S.B. Sapkal, G.K. Kakade, B.B. Shingate, M.S. Shingare, Green Chem. Lett. Rev. 3 (2010) 27–32.
[10] N. Rahmat, A.Z. Abdullah, A.R. Mohamed, Renewable Sustainable Energy Rev. 14 (2010) 987–1000.
[11] J.A. Melero, G. Vicente, G. Morales, M. Paniagua, J. Bustamante, Fuel 89 (2010) 2011–2018.
[12] C.-H. Zhou, J.N. Beltramini, Y.-X. Fan, G.Q. Lu, Chem. Soc. Rev. 37 (2008) 527–549.
[13] Y. Takagai, A. Shibata, S. Kiyokawa, T. Takase, J. Colloid Interface Sci. 353 (2011) 593–597.
[14] C. Zhang, Z. Fu, Y.C. Liu, B. Dai, Y. Zou, X. Gong, Y. Wang, X. Deng, H. Wu, Q. Xu, K.R. Steven, D. Yin, Green Chem. 14 (2012) 1928–1934.
[15] Y. Bao, J. Ma, Y. Sun, Carbohydr. Polym. 88 (2012) 589–595.
[16] M.-F. Li, S.-N. Sun, F. Xu, R.-C. Sun, Eur. Polym. J. 47 (2011) 1817–1826.
[17] P. Meenakshi, S.E. Noorjahan, R. Rajini, U. Venkateswarlu, C. Rose, T.P. Sastry, Bull. Mater. Sci. 25 (2002) 25–29.
[18] S. Saxena, S. Garg, A.K. Jana, J. Environ. Res. Dev. 6 (2012) 424–431.
[19] C. Demirbilek, C.ö. Dinç, Carbohydr. Polym. 90 (2012) 1159–1167.
[20] K.-I. Furuhata, H.-S. Chang, N. Aoki, M. Sakamoto, Carbohydr. Res. 230 (1992) 151–164.
[21] L. Hermida, A.Z. Abdullah, A.R. Mohamed, J. Porous Mater. 19 (2012) 835–846.
[22] S.H. Zeronian, M.K. Inglesby, Cellulose 2 (1995) 265–272.
[23] X. Liao, Y. Zhu, S-G. Wang, H. Chen, Y. Li, Appl. Catal., B: Environ. 94 (2010) 64–70.
[24] I. Kim, J. Kim, D. Lee, Appl. Catal., B: Environ. 148–149 (2014) 295–303.
[25] Y. Habibi, L.A. Lucia, O.J. Rojas, Chem. Rev. 110 (2010) 3479–3500.
[26] Y. Peng, D.J. Gardner, Y. Han, Cellulose 19 (2012) 91–102.
[27] Dosuna-Rodríguez, E.M. Gaigneaux, Catal. Today 195 (2012) 14–21.